

Particle simulation of AE statistics and fracture in concrete TPB test

Alberto Carpinteri¹, Giuseppe Lacidogna¹, Stefano Invernizzi^{1,*},
Amedeo Manuello¹

¹ Department of Structural, Geotechnical and Building Engineering, Politecnico di Torino, 10129, Torino, Italy.

* Corresponding author: Stefano.invernizzi@polito.it

Abstract We present some experimental results and numerical simulations of acoustic emissions (AE) due to damage propagation in a concrete specimen subjected to the three-point bending (TPB) test. The test is performed under Crack-mouth opening displacement control. Moreover, AE are detected by an eight sensors experimental device, which allows for signal localization and complete storing of the signal wave. The AE cumulative number, the time frequency analysis and the statistical properties of AE time series will be numerically simulated adopting the so-called “particle method strategy”. The method provides the velocity of particles in a set simulating the behavior of a granular system and, therefore, is suitable to model the compressive wave propagation and AE (corresponding to cracking) in a solid body. The localization of AE events is correctly reproduced. In addition, the Gutenberg-Richter statistics of AE events due to cracking, crucial for the evaluation of damage and remaining lifetime, were simulated and result in agreement with the experimental evidences.

Keywords Particle method, three-point bending test, acoustic emission, concrete.

1. Introduction

Damage and fracture characterizing the bending failure of heterogeneous materials such as concrete are complex processes involving wide ranges of time and length scales, from the micro- to the structural-scale. They are governed by the nucleation, growth and coalescence of microcracks and defects, eventually leading to the final collapse, and to the loss of the classical mechanical parameters, such as nominal strength, dissipated energy density and deformation at failure, as material properties [1]. Furthermore, the collapse mechanism is strongly related to the cracking pattern developing during the loading process. It changes from cracking and crushing, for slender beams, to shear failure characterized by the formation of inclined slip bands for deeper beams.

Instrumental and nondestructive investigation methods are currently employed to measure and check the evolution of adverse structural phenomena, such as damage and cracking, and to predict their subsequent developments. The choice of a technique for controlling and monitoring concrete or masonry structures is strictly correlated with the kind of structure to be analyzed and the data to be extracted [2–4].

This study addresses the three point bending test carried out in the laboratory in combination with acoustic emission (AE) monitoring. A similar approach has been already exploited in [5] attempting to link the amount of AE with the structural deflections.

In the assessment of structural integrity, the AE technique has proved particularly effective [5-7], in that it makes it possible to estimate the amount of energy released during the fracture process and to obtain information on the criticality of the process underway. Strictly connected to the energy detected by AE is the energy dissipated by the monitored structure. The energy dissipated during crack formation in structures made of quasi-brittle materials plays a fundamental role in the behavior throughout their entire life. Recently, according to fractal concepts, an ad hoc method has been employed to monitor structures by means of the AE technique [8]. The fractal theory takes into account the multiscale character of energy dissipation and the strong size effects associated with it. With this energetic approach, it becomes possible to introduce a useful damage parameter for structural assessment based on a correlation between AE activity in the structure and the corresponding activity recorded on specimens of different sizes, tested to failure by means of pure

compression tests.

In the following, the experimental results about the three-point bending configuration are also simulated numerically, exploiting a discrete element strategy. The main achievement of the present work consists in showing how the amount of cracking obtained from the numerical simulation and the experimentally detected AE events share the same temporal scaling laws

2. Experimental test

2.1. Acoustic Emission

The estimation of active cracks is of significant importance for any structural inspection. For an early warning of crack nucleation, the classification of active cracks is a great deal of the AE technique [9].

AE signals due to microcracks are detected by AE sensors attached on the surface of the concrete specimen. The signal waveforms are recorded by the AE measurement system. In order to classify active cracks, AE parameters such as rise time and peak amplitude of each signal are considered to calculate the rise angle (RA) value, defined as the ratio of the rise time (expressed in *ms*) to the peak amplitude (expressed in *V*) [9–12].

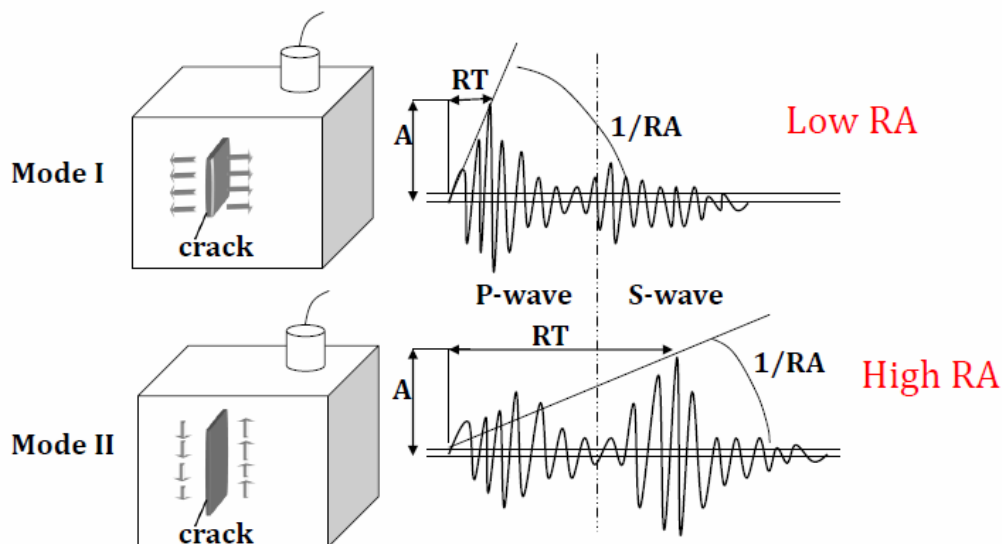


Figure 1. Typical waveforms of tensile and shear events. *A* is the amplitude and *RT* the rise time (time between the onset and the point of maximum amplitude) of the waveforms [13].

The shape of the AE waveforms is typical of the fracture mode (Fig. 1). Shear events are characterized by long rise times and usually high amplitudes, whereas low rise time values are typical of tensile crack propagations. These conditions are synthesized by the RA value.

Another parameter used to characterize the cracking mode is the Average Frequency (AF) expressed in kHz. The AF values are obtained from the AE ringdown count divided by the duration time of the signal. The AE ringdown count corresponds to the number of threshold crossings within the duration time. In general, the shift from higher to lower values of AF could indicate the shift of the cracking mode from tensile to shear [14]. Nevertheless, when a cracking process involves the opening of large cracks (Mode I), the frequency attenuation must be a function of this discontinuity. In other words, in this case the wavelength of the AE signals needs to be larger for the crack opening to be overcome, and the shift of the frequencies from higher to lower values could support

also a dominant tensile cracking mode [8].

2.2. Three-point bending test

The results of the three-point bending test performed on a beam having dimensions 100x100x840 mm (Fig. 2a) are herein reported. From the mechanical point of view, the overall behavior is characterized by a normal softening post-peak phase, as shown in Fig. 2b. The fracture energy, evaluated according to the RILEM recommendations [15], is equal to 0.124 N/mm. The corresponding total dissipated energy is equal to 0.62 J.

The evolution of the applied load, and of recorded AE with time is shown in Fig.3. The AE average frequencies range between 180 kHz and 150 kHz (Fig. 4a). A shift in frequencies from higher to lower values (Fig. 4a) and a significant decrease in RA values (Fig. 4b) after the peak load are observed (Fig. 4b). The evolution of the damage from the initial notch towards a Mode I crack is proved both by the RA and the AF decrease.

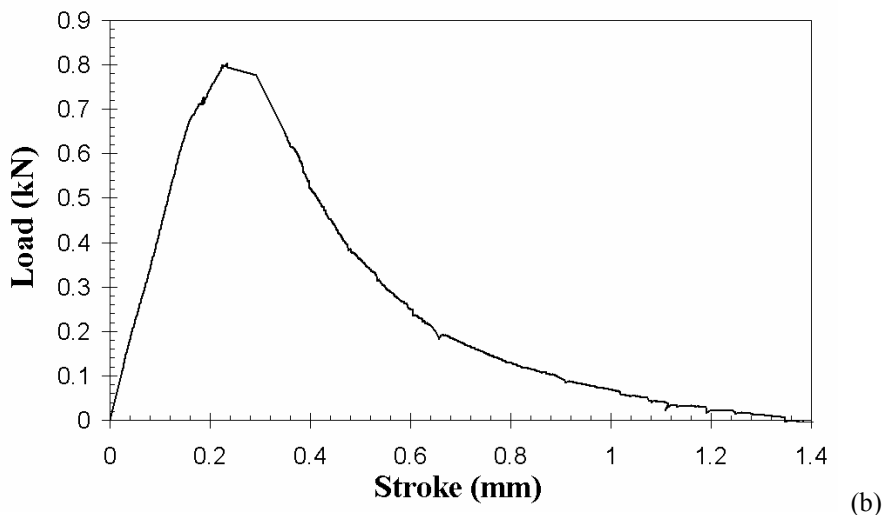


Figure 2. Three-point bending test: (a) experimental setup; (b) load vs. deflection curve.

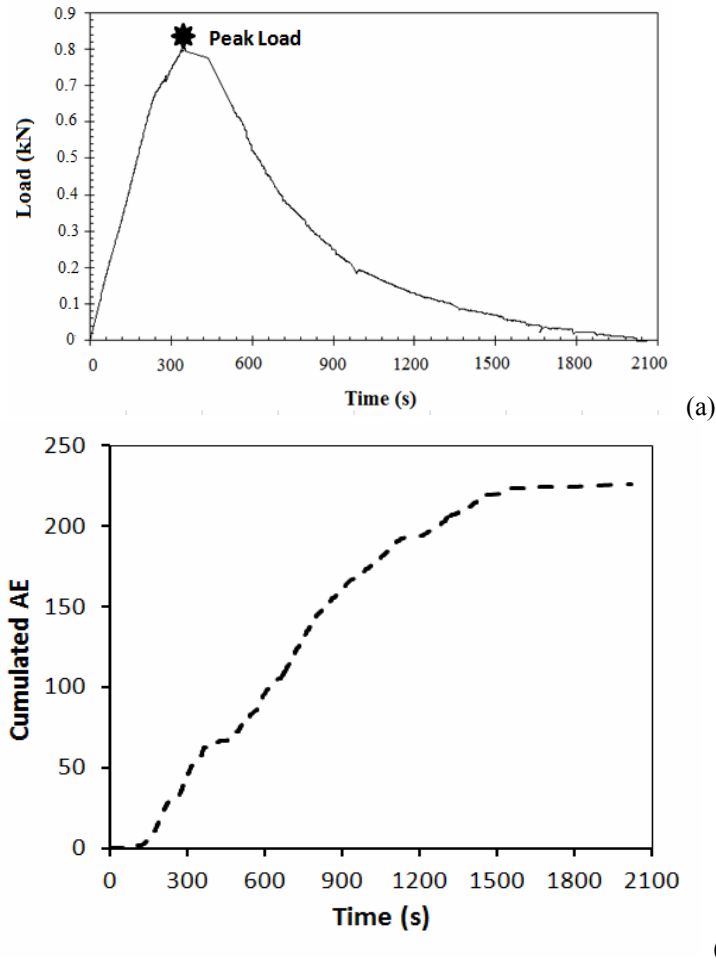


Figure 3. Three-point bending test: (a) load vs. time; (b) cumulated AE events vs. time.

The RA values obtained from the three-point bending test are considerably higher than what is obtained in case of small specimens (e.g. compression tests on cylindrical specimens [16]): as a matter of fact the additional propagation distance from AE sources to sensors, considering attenuation mechanisms, involves an increase in AE signals rise time [13]. Since the longitudinal waves are the fastest type, the delay in each AE signal between longitudinal and shear waves grows with the increasing of the propagation length, and consequently the RA rises from lower to higher values.

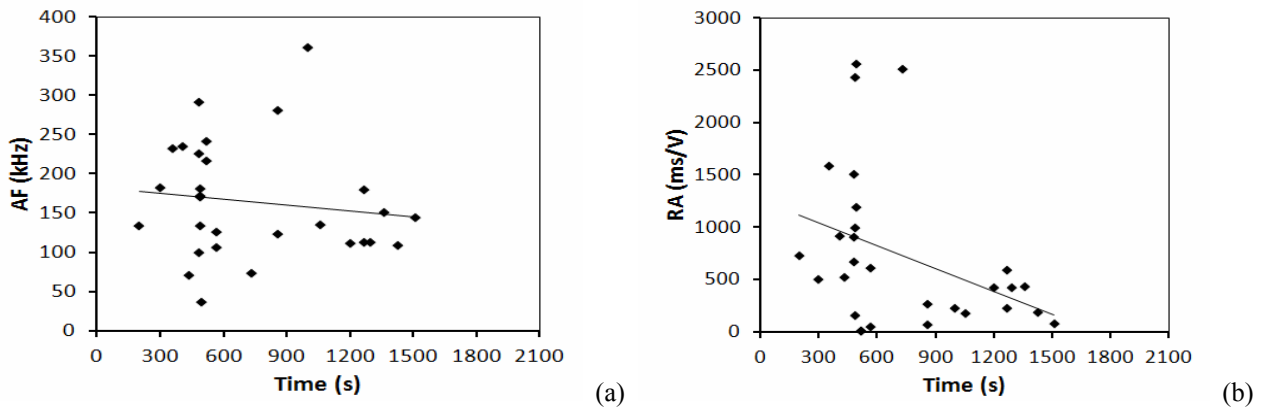


Figure 4. Three-point bending test: (a) AF values vs. time; (b) RA values vs. time;

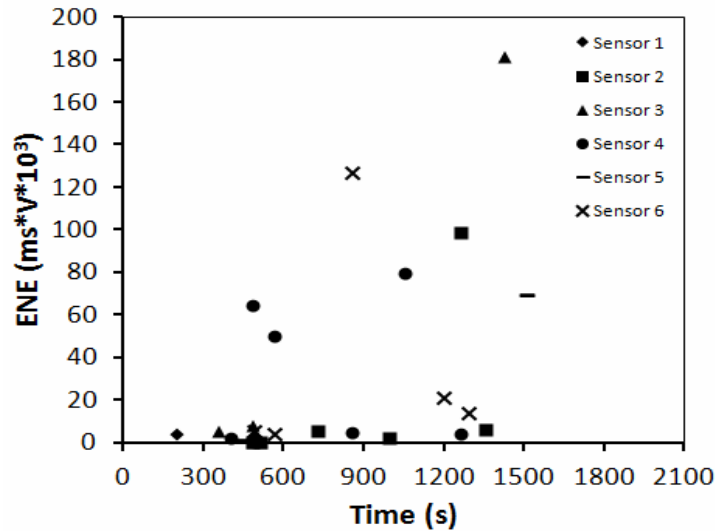


Figure 5. AE signal energy vs. time.

The signal energies of the AE events detected during the test are reported in Fig. 5, distinctly for each sensor. The average value of the total released AE signals energy is estimated as $126 \cdot 10^3 \text{ msV}$.

3. Particle simulations

The simulations have been carried out with ESyS-Particle, an open source implementation of the Distinct Element Method [17]. ESyS-Particle has been developed in-house within the Earth Systems Science Computational Centre (ESSCC) at the University of Queensland [18] since 1994. The simulation is based on direct integration of the Newton's motion equations with the Verlet algorithm. The normal interaction between colliding particles is linear and proportional to the particle small overlapping, whereas Coulomb friction, with both static and dynamic friction coefficients, rules the tangential interaction. In addition, bonded links are established between neighbor particles, according to the scheme in Figure 6. The bonded link is elastic perfectly brittle. The rupture of the bond is based on a fracture criterion that accounts for the axial, shear, torsion and bending behavior. The particles are filled together with the random packing algorithm LSMGenGeo [18], on the base of the maximum and minimum particle radius, which in our case correspond respectively to the maximum and minimum concrete aggregate radius (i.e. $r_{\max}=7.5 \text{ mm}$, $r_{\min}=1.5 \text{ mm}$).

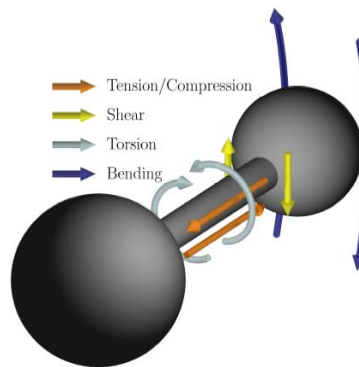


Figure 6. Scheme of the bonded interaction between two particles .

An exclusion method provides that once the bonded link is broken, the frictional interaction takes place between the neighbor particles. When the maximum and minimum radius of particles are quite different, experience shows that a power-law size distribution is obtained, providing a good approximation of the actual concrete aggregate size distribution. The bending moment is applied to the specimen by means of moving planes, provided that the particles closer to the platens were bonded to the moving planes.

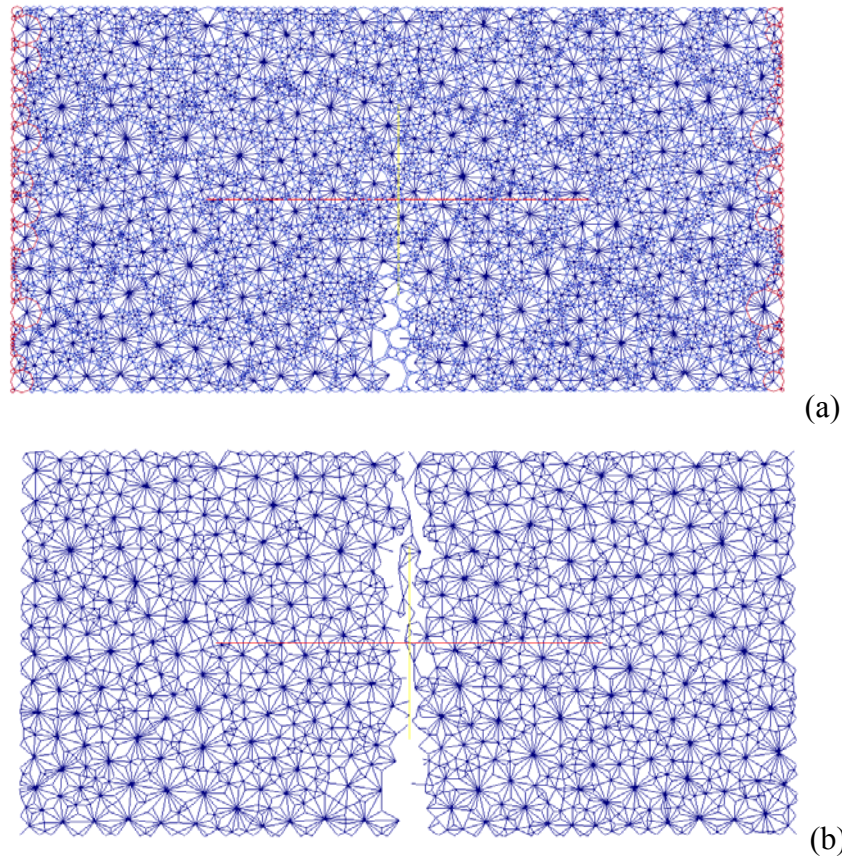


Figure 7: Three point bending test: initial configuration (a); final configuration (b).

The simulations are carried out at a fixed maximum strain velocity equal to 10^{-4} s^{-1} . A viscous type damping, proportional to the particle velocity is introduced in the simulation. The choice of the damping coefficient (in our case equal to 0.02) is based on the minimum value that regularizes the simulation without affecting the stress-strain behavior.

The position and velocity of each particle during the simulation can be recorded at a certain integration time.

In order to limit the model complexity and the computational needs, a two-dimensional simulation of three-point bending test and AE acquisition [12] has been performed. The particle discretization was limited to the central region of the beam, where almost uniform bending was simulated imposing the rotation of the extreme sections (shown in red in Fig. 7a). The initial notch is obtained removing the corresponding bonds. As soon as the bonds between particles reach the failure limit, they are removed, and the crack proceeds to the extrados of the beam (Fig. 7b).

In the present study, special attention was paid to the simulation of the temporal scaling of the acoustic emission, rather than to provide a detailed interpretation of the experimental test. Nevertheless, the mechanical parameters adopted in the analysis were chosen to better interpolate the experimental strength in the whole dimensional range.

4. Comparison between numerical and experimental AE statistics

Since the studies of Mogi and Scholz [19,20] on AE, we know that the Gutenberg-Richter empirical law can be observed at the laboratory sample scale. They showed that a significant overlap exists between the definition of AE and earthquake. This is further reinforced by the evidence that brittle fracture obeys similar statistics from tectonic earthquakes to the dislocation movements smaller than micron size. Moreover, in recent years, experiments employing acoustic emission have established remarkable results concerning the model of process zone and the quasistatic fault growth. Such experiment-based knowledge is expected to be useful for studying the fundamental behavior of natural earthquakes, because it is widely accepted that fault systems are scale-invariant [21, 22] and there exist universal similarities between faulting behaviors, from small-scale microcracking to large-scale seismic events. For example, AE events caused by microcracking activity [19–23] and stick-slip along a crack plane [24, 25] are similar to those generated by natural earthquakes.

By analogy with seismic phenomena, in the AE technique the magnitude may be defined as follows [26, 27]:

$$m = \text{Log} A_{\max} + f(r), \quad (4)$$

where A_{\max} is the amplitude of the signal expressed in μV and $f(r)$ is a correction coefficient whereby the signal amplitude is taken to be a decreasing function of the distance r between the source and the AE sensor. In seismology, the Gutenberg-Richter empirical law [28]:

$$\text{Log} N(\geq m) = a - bm, \quad (5)$$

expresses the relationship between magnitude and total number of earthquakes in any given region and time period, and is the most widely used statistical relation to describe the scaling properties of seismicity. In Eq. (5), N is the cumulative number of earthquakes with magnitude $\geq m$ in a given area and within a specific time range, while a and b are positive constants varying from a region to another and from a time interval to another. Eq. (5) has been used successfully in the AE field to study the scaling laws of AE wave amplitude distribution. This approach evidences the similarity between structural damage phenomena and seismic activities in a given region of the Earth, extending the applicability of the Gutenberg-Richter law to structural engineering [29].

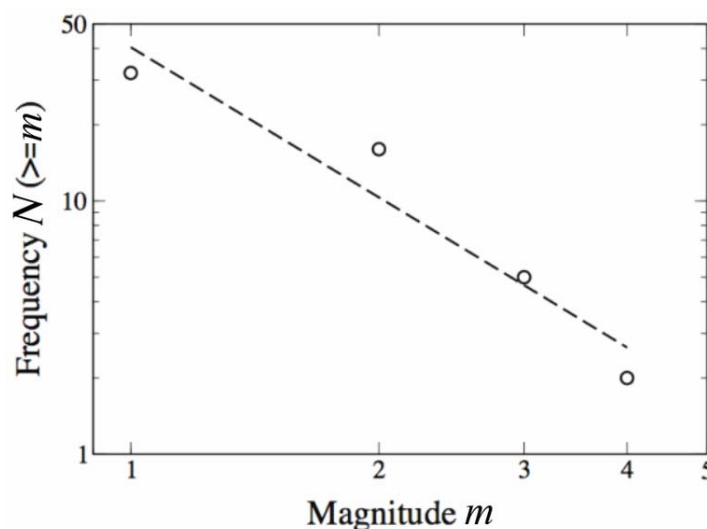


Figure 10: Frequency magnitude bilinear diagram: $a=40.4$, $b=1.97$.

The magnitude of each event is obtained summing up the number of bonds broken in each non-overlapping time window, in this case equal to 300 time steps. Finally, the frequency of the magnitude events that overcame a certain value m is reported in the classical Gutenberg-Richter chart (Figure 7c). It is worth noting that, in agreement with the experimental acquisition [29], the computed frequencies are aligned on a straight line. The slope of this line, which corresponds to the b value, is higher than the experimental value, and equal to 1.97. Further analyses are necessary to investigate the effect of the simulation dimensionality, and to obtain a better parameter calibration of the model.

5 CONCLUSIONS

The AE results obtained from the three-point bending tests, prove that the variation of the AE parameters during the loading process strictly depends on the specimen damage: a decrease in frequency may be provoked both by dominant shear cracking process and by dominant tensile cracking process. Therefore, the two different cracking modes have to be discriminated through a different AE parameter, such as the rise angle (RA), that is defined as the ratio of the rise time to the peak amplitude of each signal. Low RA values suggest a Mode I crack propagation, whereas high RA values are obtained in case of Mode II crack propagation. All the monitored damage processes display an increase in AE signal energy content approaching the final failure.

The preliminary distinct element numerical simulation of the AE statistics in the three-point bending test showed a good qualitative simulation of the Gutenberg-Richter law. Further analyses are necessary to investigate the effect of the simulation dimensionality, and to obtain a better parameter calibration of the model.

Acknowledgements

The financial support provided by the Regione Piemonte (Italy) RE-FRESCOS Project, is gratefully acknowledged.

References

- [1] A. Carpinteri, M. Corrado and G. Lacidogna, Three different approaches for damage domain characterization in disordered materials: Fractal energy density, b -value statistics, renormalization group theory. *Mechanics of Materials*, 53 (2012) 15–28.
- [2] A. Carpinteri, P. Bocca, *Damage and Diagnosis of Materials and Structures*, Pitagora Editrice, Bologna, Italy 1991.
- [3] S. Invernizzi, G. Lacidogna, A. Manuello, A. Carpinteri. AE monitoring and numerical simulation of a two-span model masonry arch bridge subjected to pier scour. *Strain*, 47:2 (2011) 158–169.
- [4] A. Anzani, L. Binda, A. Carpinteri, S. Invernizzi, G. Lacidogna, A multilevel approach for the damage assessment of historic masonry towers. *Journal of Cultural Heritage*, 11 (2010) 459–470.
- [5] A. Carpinteri, S. Invernizzi, G. Lacidogna, Structural assessment of a XVIIth century masonry vault with AE and numerical techniques, *International Journal of Architectural Heritage*, 1(2), (2007) 214–226.
- [6] A. Carpinteri, G. Lacidogna, A. Manuello, S. Invernizzi, L. Binda, Stability of the vertical bearing structures of the Syracuse Cathedral: Experimental and numerical evaluation. *Materials & Structures*, 42 (2009) 877–888.
- [7] A. Carpinteri, S. Invernizzi, G. Lacidogna, In situ damage assessment and nonlinear modelling of an historical masonry tower. *Engineering Structures*, 27 (2005) 387–395.
- [8] A. Carpinteri, G. Lacidogna, N. Pugno, Structural damage diagnosis and life-time assessment by acoustic emission monitoring, *Engineering Fractures Mechanics*, 74 (2007) 273–289.

- [9] C. Grosse and M. Ohtsu, *Acoustic Emission Testing*, Springer 2008.
- [10] RILEM Technical Committee TC212-ACD, Acoustic Emission and related NDE techniques for crack detection and damage evaluation in concrete: Measurement method for acoustic emission signals in concrete. *Mater. Struct.*, 43 (2010) 1177–81.
- [11] RILEM Technical Committee TC212-ACD, Acoustic Emission and related NDE techniques for crack detection and damage evaluation in concrete: Test method for damage qualification of reinforced concrete beams by Acoustic Emission. *Mater. Struct.* 43 (2010) 1183–6.
- [12] RILEM Technical Committee TC212-ACD, Acoustic Emission and related NDE techniques for crack detection and damage evaluation in concrete: Test method for classification of active cracks in concrete by Acoustic Emission. *Mater. Struct.* 43 (2010) 1187–9.
- [13] D.G. Aggelis, A.C. Mpalaskas, D. Ntalakas and T.E. Matikas, Effect of wave distortion on acoustic emission characterization of cementitious materials. *Construction and Building Materials*, 35 (2012) 183–190.
- [14] K. Ohno, M. Ohtsu, Crack classification in concrete based on Acoustic Emission. *Constr. Build. Mater.* 24 (2010) 2339-46.
- [15] RILEM 50-FMC Committee, Determination of the fracture energy of mortar and concrete by means of three-point bend tests on notched beams. *Mater. Struct.* 18 (1986) 286-90.
- [16] G. Lacidogna, F. Accornero, M. Corrado, and A. Carpinteri, Crushing and fracture energies in concrete specimens monitored by Acoustic Emission, VIII International Conference on Fracture Mechanics of Concrete and Concrete Structures, FraMCoS 8, Toledo, Spain, March 10-14, 2013.
- [17] <https://twiki.esscc.uq.edu.au/bin/view/ESSCC/ParticleSimulation>
- [18] <https://launchpad.net/esys-particle/>
- [19] K. Mogi, Magnitude frequency relations for elastic shocks accompanying fractures of various materials and some related problems in earthquakes”, *Bull. Earthquake Res. Inst. Univ. Tokyo*, 40 (1962) 831–853.
- [20] C. H. Scholz, The frequency-magnitude relation of microfracturing in rock and its relation to earthquakes, *Bull. Seismol. Soc. Am.*, 58 (1968) 399–415.
- [21] T. Hirata, “Fractal dimension of fault system in Japan: fracture structure in rock fracture geometry at various scales”, *Pure Appl. Geophys.* 131 (1989) 157–170.
- [22] E. Bonnet, O. Bour, N.E. Odling, P. Davy, I. Main, P. Cowie, B. Berkowitz, “Scaling of fracture systems in geological media”, *Rev. Geophys.* 39 (2001) 347–383.
- [23] D.A. Lockner, J.D. Byerlee, V. Kuksenko, A. Ponomarev, A. Sidorin, “Quasi static fault growth and shear fracture energy in granite”, *Nature* 350 (1991) 39–42.
- [24] N. Kato, K. Yamamoto, T. Hirasawa, Microfracture processes in the break down zone during dynamic shear rupture inferred from laboratory observation of near-fault high-frequency strong motion, *Pure Appl. Geophys.* 142 (1994) 713–734.
- [25] X.L. Lei, O. Nishizawa, K. Kusunose, A. Cho, T. Satoh, On the compressive failure of shale samples containing quartz-healed joints using rapid AE monitoring: the role of asperities, *Tectonophysics* 328 (2000) 329–340.
- [26] S. Colombo, I.G. Main, M.C. Forde, Assessing damage of reinforced concrete beam using “*b*-value” analysis of acoustic emission signals, *J. Mat. Civil Eng. (ASCE)* 15 (2003) 280–286.
- [27] M.V.M.S. Rao, P.K.J. Lakschmi, Analysis of *b*-value and improved *b*-value of acoustic emissions accompanying rock fracture, *Curr. Sci. – Bangalore* 89 (2005) 1577–1582.
- [28] C.F. Richter, *Elementary Seismology*. W.H. Freeman, San Francisco 1958.
- [29] S. Invernizzi, A. Carpinteri, G. Lacidogna, Particle-based numerical modeling of AE statistics in disordered materials, *Meccanica*, 48:1 (2013) 211–220.